Measurement report: Underestimated reactive organic gases from residential combustion: insights from a near-complete speciation

4 Yaqin Gao[1], Hongli Wang[1]*, Lingling Yuan[1], Shengao Jing[1], Bin Yuan[2], Guofeng Shen[3],
5 Liang Zhu[4,5], Abigail Koss[5], Yingjie Li[1], Qian Wang[1], Dan Dan Huang[1], Shuhui Zhu[1],
6 Shikang Tao[1], Shengrong Lou[1], Cheng Huang[1]*

7 [1] State Environmental Protection Key Laboratory of Formation and Prevention of
8 Urban Air Pollution Complex, Shanghai Academy of Environmental Sciences,
9 Shanghai 200233, China

10 [2] Institute for Environmental and Climate Research, Jinan University, Guangzhou
11 511443, China

12 [3] Laboratory of Earth Surface Processes, College of Urban and Environmental Science,
13 Peking University, Beijing 100871, China

14 [4] Tofwerk China, Nanjing 210000, China

15 [5] Tofwerk AG, Thun 3645, Switzerland

16 * Corresponding author: Hongli Wang, E-mail: wanghl@saes.sh.cn; Cheng Huang, E-
17 mail: Huangc@saes.sh.cn

Abstract

Reactive organic gases (ROGs), as important precursors of secondary pollutants, are not well resolved as the chemical complexity challenged its quantification in many studies. Here, a near-complete speciation of ROGs with 125 species was developed and applied to evaluate their emission characteristics from residential solid fuel combustion. ROGs identified by the present method accounted for ~90% of the "total" as the sum of species by Gas Chromatography equipped with a Mass Spectrometer and a Flame Ionization Detector (GC-MS/FID) and H_3O^+/NO^+ Proton Transfer Reaction Time-of-Flight Mass Spectrometer (Vocus PTR-ToF-MS). The study further revealed that with 55 species, mainly oxygenated species, higher hydrocarbons with > 8 carbon atoms, and nitrogen-containing ones, previously un- and under-characterized, ROG emissions from residential coal and biomass combustion were underestimated by 44.3% ± 11.8% and 22.7% ± 3.9%, respectively, which further amplified the underestimation of secondary organic aerosols formation potential (SOAP) as high as 70.3% ± 1.6% and 89.2% ± 1.0%, respectively. The OH reactivity (OHR) of ROG emissions was also undervalued significantly. The study highlighted the importance of acquiring

34   completely speciated measurement of ROGs from residential emissions, as well as

35   other processes.

36

37   **Highlights**

38   A near-complete speciation of ROGs emitted from residential combustion was

39   developed.

40   Oxygenated species, higher hydrocarbons and nitrogen-containing ones played larger

41   roles in the emissions of residential combustion comparing with the common

42   hydrocarbons.

43   ROG emissions from residential combustion were largely underestimated, leading more

44   underestimation of their OHR and SOAP.

45

46   **Keywords:** Chemical speciation, Reactive organic gases, Residential combustion,

47   Estimation bias

1. Introduction

48

49   Residential combustion, dominated by approximately 89% solid fuels in China
50   (Zhu et al., 2019), is responsible for ~23% and ~71% of the outdoor and indoor $PM_{2.5}$
51   concentrations, and ~67% of $PM_{2.5}$-induced premature deaths (Yun et al., 2020).
52   Reactive organic gases (ROGs), organic gases other than methane, from residential
53   combustion, have been shown to serve as key precursors for secondary organic aerosols
54   (SOA) (Huo et al., 2021) and ozone formation (Heald and Kroll, 2020; Heald et al.,
55   2020). Recommended 56 hydrocarbon species according to the Photochemical
56   Assessment Monitoring Station (PAMS), the most common ROG species, have been
57   recognized as the dominant ROGs from residential combustion in past years (Mo et al.,
58   2016). With the development of advanced detection technologies, more ROGs like
59   oxygenated volatile compounds (OVOCs) and higher alkanes with carbon atoms more
60   than 12, have been found to play important roles in the source emissions as well as in
61   the atmospheric chemistry (Yuan et al., 2017; Wang et al., 2020a; Chang et al., 2022;
62   Gao et al., 2022; Wang et al., 2022; Qu et al., 2021). A more complete chemical
63   description of ROGs emitted from residential coal and biomass combustion was
64   critically important to get more insights into their atmospheric effects.

65   Several studies attempting complete identification and quantification of ROGs
66   mainly emitted from biomass combustion have been conducted in the laboratory using
67   multiple trace-gas instruments in recent years (Gilman et al., 2015; Hatch et al., 2017),
68   which have mainly focused on emissions from various trees and other wildfire fuels.
69   Andreae (Andreae, 2021, 2019) summarized the ROG speciation and emission factors
70   of various kinds of combustion processes and concluded there were lack of results from
71   actual combustion processes like in field or household combustion and species such as
72   higher alkanes serving as important SOA precursors were not included in the previous
73   studies (Table S1)(Koss et al., 2018; Cai et al., 2019).

74   In this study, the ROGs emitted from typical Chinese household stoves with six
75   kinds of solid fuels were analyzed with the combination of a high mass resolution Vocus
76   Proton Transfer Reaction Time-of-Flight Mass Spectrometer (Vocus PTR-ToF-MS)
77   under two kinds of ion source (H_3O^+ / NO^+) and a gas chromatography system equipped
78   with a mass spectrometer and a flame ionization detector (GC-MS/FID). The Vocus

79   PTR-ToF-MS have a good sensitivity for most of OVOCs and aromatics as well as

80   some nitrogen-/sulfur-containing species in the mode of H_3O^+ (Wu et al., 2020), and

81   for higher alkanes in NO^+ mode (Wang et al., 2020a). GC-MS/FID has a wide detection

82   range of organics, and here is used for the detection of nonmethane hydrocarbons

83   (NMHCs) and some carbonyls. Accordingly, a near-complete speciation of ROGs

84   including 125 species results from the combined instrument data sets, further

85   supporting the evaluation of the roles of ROG emissions from residential combustion

86   in the formation potential of SOA and ozone in China.

2. Materials and methods

2.1 Sampling

89   The ROG samples of the combustion of four typical biomass fuels (wood, corncob,

90   bean straw and corn straw) and two typical coals (anthracite, and briquette coals) (see

91   Fig. S1) were collected from the stack nozzles of household stoves by vacuumed

92   SUMMA canisters (Entech Inc., 3.2 L). During canister sampling, the combustion in

93   the stoves was in the stage of flaming visually, which was the common condition for

94   heating or cooking in the rural areas in northern China. Particles was removed by a

95   particle-filter with 5.0 μm pore size Teflon filter (PTFE). Temperatures (37 ± 17 °C) of

96   flue gas were monitored at the sampling location by a flue gas analyzer (Testo 350).

97   Wood and straws burned at an average temperature of 394°C (in the range of 231°C–

98   567°C) and 353°C (334°C–371°C), respectively, while the residential coals burned at a

99   higher temperature (514°C, 411°C–581°C), which were measured by an

100   infrared thermometer in the stove. There were 23 samples were collected in all in this

101   study, as shown in Fig. S1.

2.2 Analysis

103   All the samples stored in SUMMA canisters were detected with the combination

104   of Vocus PTR-ToF-MS (Vocus 2R, Tofwerk AG, Switzerland) and GC-MS/FID (TH-

105   300, Wuhan Tianhong Instruments, China) within 9 days. The effect of storage inside

106   the canister was evaluated using the standard samples with different storage duration in

107   the laboratory. The intercomparisons of different methods were carried out to ensure

108   the results were comparable. Accordingly, the measurement uncertainties of different

109   ROG species were estimated, as listed in Table S2. Details of the measurements were

110   as following.

111   **PTR-ToF-MS.** A commercial Vocus PTR-ToF-MS with H_3O^+ and NO^+ chemistry

112   was used to detect ROGs. The Vocus PTR-ToF-MS was operated at a mass resolving

113   power of 10000 m Δm^{-1} (full width at half maximum, FWHM). A total of 1005 peaks

114   were extracted from raw spectral data by Tofware package v3.2.3 (Tofwerk Inc.),

115   including all peaks with mass to charge ratio (m/z) below 200 under H_3O^+ mode and

116   selected peaks under NO^+ mode (mainly higher alkanes). The peak assignment was

117   derived based on accurate m/z values, isotopic patterns and previous study results

118   (Pagonis et al., 2019). In all, 162 ions with a relative high degree of certainty

119   associated with previous reports (Pagonis et al., 2019; Cai et al., 2019; Koss et al., 2018)

120   were identified and had noticeable concentrations in the samples. These 162 masses

121   represent about 89% of the total extracted signal measured by Vocus PTR-ToF-MS,

122   assuming all the signals with the same sensitivity as acetone. Twenty-six out of 162

123   identified species were calibrated using customized cylinders (Linde Gas North

124   America LLC, USA) including benzene, toluene, styrene, m-xylene, 1,3,5-

125   trimethylbenzene, isoprene, alpha-pinene, methyl vinyl ketone, naphthalene, acrolein,

126   acetone, methyl ethyl ketone, 2-pentanone, acetaldehyde, furan, acetonitrile,

127   dichlorobenzene, ethyl acetate and $C_8–C_{15}$ n-alkanes. More details of the calibration

128   could be found in our previous studies (Gao et al., 2022; Wang et al., 2020b).

129   Sensitivities of $C_{16}–C_{21}$ alkanes were assumed to be same as that of C_{15} n-alkane

130   according to Wang et al.(2022) (Wang et al., 2020a). For other measured species, we

131   used the method proposed by Sekimoto et al. (2017) to determine the relationship

132   between ROG sensitivity and kinetic rate constants for proton transfer reactions of

133   H_3O^+ with ROGs (Fig. S2), and the uncertainties of the concentrations for these

134   uncalibrated species were about 50% (Table S1) (Sekimoto et al., 2017).

135   **GC-MS/FID.** 57 NMHCs and 11 carbonyls were detected by GC-FID/MS

136   coupled with a cryogen-free preconcentration device, which were calibrated by gas

137   standards (Linde Gas North America LLC, USA) including 68 species as listed in Table

138   S2. Intercomparisons between GC-FID/MS and Vocus PTR-ToF-MS for overlapped

139   ROG species were carefully evaluated. Good agreements for aromatics and some

140   carbonyls were observed in all samples (Fig. S3).

141   **Loss in storage.** To determine the possible artifacts caused by the SUMMA
142   canister storage, standard samples with concentration of 5 ppbv containing 81 species
143   were prepared into clean vacuum SUMMA canisters and detected within 2h as well as
144   on days 1, 2, 4, 7, 10 and 14 after preparation. The detailed compounds and deviations
145   were shown in Table S2 and Fig. S4. Generally, on the 10th day, the relative deviations
146   were within 20% for 71 out of the 81 standard compounds, and the rest 10 compounds
147   like diethylbenzene, terpenoids and long-chain alkanes had the relative deviations
148   within 49%. The concentration of the standard sample was lower than most of the
149   concentrations of species in source samples. Thus, the estimated loss in the storage in
150   this study was the upper bound for the source samples. For acids and alcohols with
151   larger loss in the canisters potentially due to the functional groups of -COOH and -OH,
152   the measured concentrations in the samples were excluded from the results, and
153   especially there were no standard gases used to evaluate the loss during storage. The
154   estimated total uncertainty of ROGs were in the range of 4%–50%, which included the
155   uncertainties of storage and detection, as listed in Table S2.

156   **Speciation.** Finally, 87 out of the 162 species measured by Vocus PTR-ToF-MS
157   were used in this study, including 31 overlapped species with those by GC-FID/MS
158   (Fig. 1). Since isomers can't be distinguished by Vocus PTR-ToF-MS, GC-FID/MS
159   measured concentrations for overlapped ROG species were used in this study.
160   Combining with other 37 species detected by GC-MS/FID, a total of 124 species were
161   used in this study, including 27 alkanes, 9 alkenes, 1 alkyne, 16 aromatics, 6 biogenic
162   volatile organic compounds (BVOCs), 9 polycyclic aromatic hydrocarbons (PAHs), 14
163   higher alkanes, 15 carbonyls, 10 furans (furan and its homologues and derivatives), 9
164   phenols (phenol and its homologues and derivatives) and 8 nitrogen-containing
165   compounds. Other species detected by Vocus PTR-ToF-MS but not included in the
166   follows were mainly acids, alcohols and species with more than 2 oxygen atoms,
167   accounting for about 8% (ranging from 2% to 17% in different samples) of the total
168   ROG masses as shown in Fig. S5.

169   **Formaldehyde**, a very important species from combustion (Zarzana et al., 2017)
170   but not measured in this study, was assumed to account for ~7% and ~5% in all

171 discussed species for coal and biomass combustion in this study, respectively, according
172 to the previous reported results (Cai et al., 2019; Stockwell et al., 2015; Stockwell et
173 al., 2016). Specifically, the emission ratio of formaldehyde (ER$_{HCHO, ref}$) from anthracite
174 coal combustion (2.13 g/g,benzene) and straws (2.85 g/g,benzene) could be obtained
175 from Cai et al. (2019) and Stockwell et al. (2016). Considering the emission ratio of the
176 species covered by both previous studies and the current work were consistent as shown
177 in Fig. S6, the mass fraction of formaldehyde ($f_{HCHO,cal}$) in ROG emissions from coal
178 combustion of this work could be calculated using the previously reported ER$_{HCHO, ref}$
179 and the currently measured mass fraction of benzene ($f_{benzene}$) as follows:

180
$$f_{HCHO,cal} = \frac{ER_{HCHO,ref} \times f_{benzene}}{1 + ER_{HCHO,ref} \times f_{benzene}}$$
(1)

181 Finally, all the species included in this study were sketched in Fig. 1, as well as
182 their mass fractions in ROG emissions from residential combustion which would be
183 discussed in detail below. Briefly, although only 125 out of more than 1000 species
184 were included in the speciation of ROGs from residential combustion emissions, they
185 have contributed 89±20% and 92±11% of the total ROGs from residential combustion.
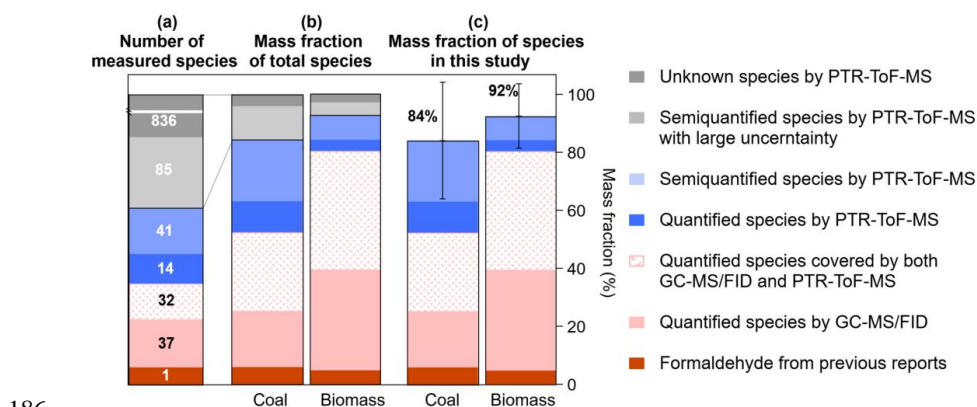
186

187 **Figure 1.** The number and mass fraction of species measured by GC-MS/FID and
188 Vocus PTR-ToF-MS. (a) Number of measured species by GC-MS/FID and Vocus PTR-
189 ToF-MS. (b) Average mass fraction of all measured species from coal combustion and
190 biomass combustion samples. (c) Mass fraction of selected 125 species in this study.
191 The result of formaldehyde was cited from previous studies (Cai et al., 2019; Stockwell

192   et al., 2015). All the quantified species were calculated by standard matters. The

193   semiquantified species were measured by Vocus PTR-ToF-MS (H_3O^+) by the method

194   proposed by Sekimoto et al. (2017) to determine the relationship between ROG

195   sensitivity and kinetic rate constants for proton transfer reactions of H_3O^+ with ROGs.

196   Among the above semiquantified species, species with the functional groups of -OH

197   and -COOH as well as those with more than two oxygen atoms had relatively large

198   uncertainty due to the potential loss in the storage. The unknown species were detected

199   by Vocus PTR-ToF-MS (H_3O^+) and were semiquantified by the sensitivity of acetone.

200   **3. Results and discussions**

201   **3.1 A near-complete speciation of ROGs from residential combustion**

202   ROG compositions emitted from typical residential combustion using two types of

203   coals (anthracite, and briquettes) and four types of biomasses (wood, corncob, corn

204   straw and bean straw) are shown in Fig. 2. The measured ROG profiles for each kind

205   of fuel had a good correlation (R > 0.6) (Fig. S7), and the average result was used here.

206   Generally, ROGs emitted from the residential combustion can be divided into three

207   groups based on the element composition, including hydrocarbons, oxygenated species,

208   and nitrogen-containing species. Differing from the previously studies which mainly

209   stressed the dominant role of hydrocarbons (Mo et al., 2016; Stockwell et al., 2015;

210   Wang et al., 2014), the contribution of oxygenated species (36.8%–56.8%) was

211   comparable with that of hydrocarbons (40.8%–48.7%) in this study. It was expected as

212   24 more oxygenated species mainly including furans, phenols and carbonyls were

213   measured by Vocus PTR-ToF-MS in our study, which were un- and under-characterized

214   in previous studies using GC methods. Besides hydrocarbons and oxygenated species,

215   nitrogen-containing species mainly included acetonitrile and acrylonitrile also played a

216   considerable role in ROG emissions from residential combustion, with the proportions

217   ranging from 5.7% to 14.5%, which have been previously reported (Cai et al., 2019).

218   Here, we defined the species previously un- and under-characterized by GC

219   methods as newly identified species and could be measured only using Vocus PTR-

220   ToF-MS in this study, and as a result 55 of 125 species were newly identified species.

221   As shown in Fig. 2, these newly identified species mainly including furans and phenols

222   contributed 44.3% ± 11.8% of the total ROGs for coal emissions and 22.7% ± 3.9% of

223   the total ROGs for biomass emissions. We also compared our results with the previous

224   reports, and for comparison the previous speciation was scaled by the total fraction of

225   the previously reported species in the total ROGs measured in this study. As shown in

226   Fig. 2 and Fig. S5, the fraction of reported species in previous studies was comparable

227   to the present result. In particular, as Fig. 2(c) shown, the present composition of ROGs

228   from residential wood combustion was close to that of Black Spruce combustion

229   simulated in laboratory by multiple advanced trace-gas instruments, which reported

230   464–551 species (~173 molecules) in all (Hatch et al., 2017). It further confirmed that

231   the obtained ROG characterization with the combination of Vocus PTR-ToF-MS and

232   GC-FID/MS were nearly complete. Our study underscored the importance of the

233   completely speciated measurement of the ROG emissions from residential combustion

234   especially for coal combustion.

235   Large difference was observed between the ROG speciation of coal and biomass

236   combustion but not significant among different types of coal or biomasses, as shown in

237   Fig. 2. Specifically, the alkenes mainly ethylene and propene dominated hydrocarbons

238   emitted from biomass combustion, while alkanes were the most hydrocarbons from coal

239   combustion. Especially, coal combustion emitted considerable higher alkanes including

240   8–21 carbon atoms and gaseous PAHs (mainly including 2–3 benzene rings), primarily

241   generated by pyrolysis of the volatile matter in coal (Du et al., 2020), accounting for

242   8.3%–14.8% of ROGs much higher than the minor fractions (0.4%–2.4%) for biomass

243   combustion emissions. In terms of oxygenated species, coal combustion emitted

244   considerable furans (16.8% ± 3.2%) and phenols (6.1% ± 1.5%) mainly formed through

245   pyrolysis of polymers in coal (Liu et al., 2017; Morgan and Kandiyoti, 2014), which

246   together played a comparable role with carbonyls (26.9% ± 6.8%) in ROGs. In

247   comparison, carbonyls (40.6% ± 6.6%) were the dominant oxygenated species in ROG

248   emissions from biomass combustion, mainly originated from products of biomass

249   pyrolysis and pyrosynthesis (Morgan and Kandiyoti, 2014). A slightly higher

250   proportion of phenols and furans from wood combustion (12.8% ± 3.0%) than straw

251   combustion (8.7% ± 2.8%) were observed, possibly resulting from the higher

252   composition of lignin in wood (Collard and Blin, 2014). Considerable terpenes were

253   also observed in ROG emissions from residential coal (1.5 ± 0.2%) and biomass (3.2%

254   ± 0.5%) combustion.
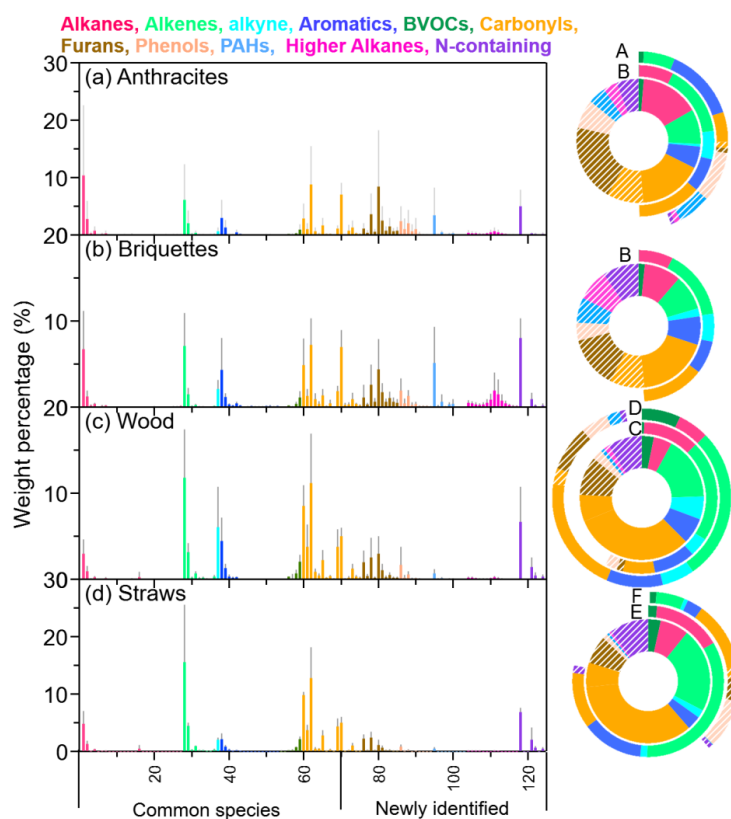
255

256   **Figure 2.** Source profiles and compositions of the four types of residential fuels

257   including (a) anthracites, (b) briquettes, (c) wood and (d) straws (average of corncob,

258   bean straws and corn straws) as well as those of the previous results. A. anthracites

259   combustion in stove from Cai et al., 2019; B. residential coal combustion simulation in

260   lab from Mo et al., 2016; C. hardwood combustion simulation in lab from Stockwell et

261   al., 2016; D. Black Spruce combustion simulation from lab experiments reported by

262   Hatch et al., 2017; E. wood combustion simulation from Wang et al., 2014; F. rice straw

263   combustion simulation from Stockwell et al., 2015 (Cai et al., 2019; Mo et al., 2016;

264   Wang et al., 2014; Stockwell et al., 2016; Hatch et al., 2017; Stockwell et al., 2015).

265   The measured species corresponding to the numbers of horizontal axis are listed in

266   Table S2. The shaded parts of pie charts represent the newly identified species.

267   **3.2. SOAP and OHR underestimation from newly identified species**

268   To further understanding the role of residential combustion emitted ROGs in

269   atmospheric chemistry, the OH reactivity (OHR) and formation potential (SOAP) of

270   per unit mass (or concentration) of ROGs emitted from residential combustion was

271   calculated based on the source profiles. OHR is defined here as the sum of OH reactivity

272   of each species, calculated by product of ROG species weight percentage (W_{ROGi}) in

273   emissions from residential combustion and corresponding OH reaction rate ($k_{OH+ROGi}$)

274   (Carter, 2008; Koss et al., 2018), as presented in Eq. (2) below. SOAP is the sum of

275   SOAP of each species and calculated by multiplying proportion of ROG species with

276   according SOA yields based on the reported approach(Ng et al., 2007; Lim and

277   Ziemann, 2009), as presented in Eq. (3) below.

278
$$OHR = \sum W_{ROGi} \times k_{OH+ROGi} \qquad (2)$$

279
$$SOAP = \sum W_{ROGi} \times Yield_{ROGi} \qquad (3)$$

280   Figure 3 shows the OHR and SOAP of per unit mass (or concentration) ROG

281   emissions. The OHR for coal and biomass emissions were quite similar (0.14–0.16 s^{-1}

282   μg^{-1} m^3) but with different compositions, which was expected as the differences of their

283   ROG compositions. The OHR was dominated by oxygenated species (39.6%–73.7%)

284   and alkenes (15.0%–48.2%), and the contribution of other species was within the range

285   of 9.3%–17.1%. The newly identified ROG species dominated the OHR of coal

286   combustion with the fractions of 64.2% ± 7.8% and 54.6% ± 9.3% for anthracites and

287   briquettes combustion, respectively, due to the large contribution of furans, phenols,

288   PAHs, and higher alkanes in ROGs. In comparisons, the previously reported species

289   contributed more to OHR of biomass combustion than that of newly identified species.

290   The ratio of OHR between newly identified and previously reported ROGs was 1.20–

291   1.80 for coals and 0.22–0.51 for biomass, much higher than the ratios of their emissions

292   (0.79–0.81 for coals and 0.20–0.36 for biomass). It meant that the OHR of ROG

293   emissions from residential coal and biomass combustion was underestimated by 59.4%

294   ± 4.8% and 26.2 ± 6.8%, respectively, without the newly identified species.

295   SOAP derived from per unit mass ROG emissions of coal combustion was 0.078–

296   0.085 μg μg^{-1}, much higher than that from biomass combustion (0.016–0.035 μg μg^{-1}).

297   Nevertheless, for all samples, newly identified ROGs accounted for over 70% of the

298   SOAP. SOAP was dominated by newly identified oxygenated species like phenols

299   which contributed 47.6% ± 12.4% and 56.7% ± 7.0% to SOAP of emissions from coal

300   and biomass combustion, respectively, and higher alkanes and PAHs also played

301   important roles in SOAP emissions from coal combustion. The ratios of SOAP derived

302   from newly identified ROGs and previously reported ROGs were 7.8–8.8 and 2.2–2.7

303   for coals and biomass, respectively, much higher than those of mass percentages. These

304   results indicated that for both coal and biomass combustion, the measurement of newly

305   identified ROGs would be greatly affected on SOA estimation. The field study has

306   found that newly identified ROGs like higher alkanes and PAHs contributed more than

307   60% of SOA formation from measured precursors in ambient air (Wang et al., 2020a).

308   Our study of ROG emissions could donate to the explanation of the high SOA formation

309   in atmosphere to some extent. In other words, failure to include newly identified ROGs

310   in emission inventories and SOA models could lead to significant underestimation of

311   residential contribution to SOA production.
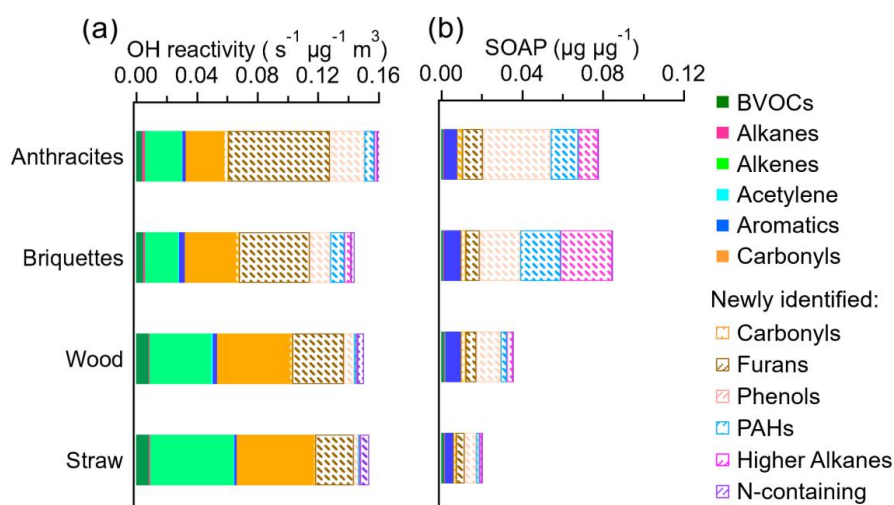
312

313   **Figure 3.** OH reactivity and SOA formation potential (SOAP) of per unit mass (or

314   concentration) of ROG emissions for coal and biomass combustion. The shaded parts

315   of bar charts represent the newly identified species.

3.3 ROG emissions from residential combustion in China

317   ROG emissions could generally be calculated through multiplying the activity data

318   by the emission factors which were not measured in this study. However, the emission

319   factors of most of the common ROGs like hydrocarbons in the emissions from

320   residential combustion have been reported in previous studies(Cai et al., 2019;

321   Stockwell et al., 2015). Hence, the emission factor of the newly identified ROG species

322   in this study could be estimated by the reported emission factor (EF) of the previously

323   reported species combining with their emission ratio (ER) in residential combustion.

324   Here, the benzene as well as its reported EF was used for the purpose above, and we

325   also tested other species with reported EFs (Fig. S8). There were no significant

326   differences (-39%–4% for straws and 6%–26% for coals) of the estimated EFs of newly

327   identified ROGs among different tests, which further confirmed our results were

328   comparable with the previous studies but with more ROG species measured, as shown

329   in Fig. S8. The ER of other ROG species to benzene was the ratio of their concentrations

330   in the sample, and the average ER in different samples of each type of fuel was used in

331   this study, as listed in Table S3. Notably, the EFs of anthracite and straw combustion

332   were used below to estimate the ROG emissions of residential coal and straw

333   combustion in China mainland.

334   Accordingly, the national ROG emissions of residential combustion were estimated

335   combining with the residential coal consumption and the crop straw combustion data

336   in China. Specifically, the data of residential coal consumption from 2010 to 2019 were

337   from the China Energy Statistical Yearbook (National Bureau of Statistics, 2010-2022),

338   which included the data of each province in China mainland in each year. The data of

339   crop straw combustion from 2010 to 2019 (Table S4) were from Report of Prospects

340   and Investment Strategy Planning Analysis on China Straw Refuse Treatment Industry

341   (2022-2027) (Qianzhan Industrial Research Institute, 2022), which only reported the

342   total amount of the whole China mainland and included both the household and field

343   combustion. The province data of crop straw combustion in 2017 (Table S5) were used

344   to study the spatial distribution in this study, which were from Second National

345   Pollution Source Census Bulletin (Ministry of Ecology and Environment of the People's

346   Republic of China et al., 2020).

347   The spatial and temporal distribution of ROG emissions from residential

348   combustion was presented in Fig. 4. The total emissions of ROGs from residential coal

349   combustion and crop straw combustion were 14 kt and 4384 kt in 2019, respectively,

350   and as expected these values were underestimated by 44.3% ± 11.8% and 22.7% ± 3.9%,

351   respectively, due to fewer species were included previously. Unexpectedly, the ROG

352   emissions from crop straw combustion were two orders of magnitude higher than those

353   of coal combustion, which included those both from household and field combustion.

354   Notably, the straw combustion emissions were stable after 2017 comparing with the

355   gradual decrease from 2010 to 2017, mainly due to the limitation of straw utilization

356   (Zhu et al., 2019). In comparison, ROG emissions of residential coal combustion began

357   to decrease after 2017 benefiting from the clean heating action in the north of China

358   (National Development and Reform Commission, 2017). Spatially, the hot areas of

359   ROG emissions from residential coal combustion were mainly in the North China Plain

360   (NCP)(Yang et al., 2020), while those of straw combustion were mainly in the main

361   food-production bases of China like the northeastern China, the southern NCP, and

362   Jiangsu, Anhui, and Hunan provinces.
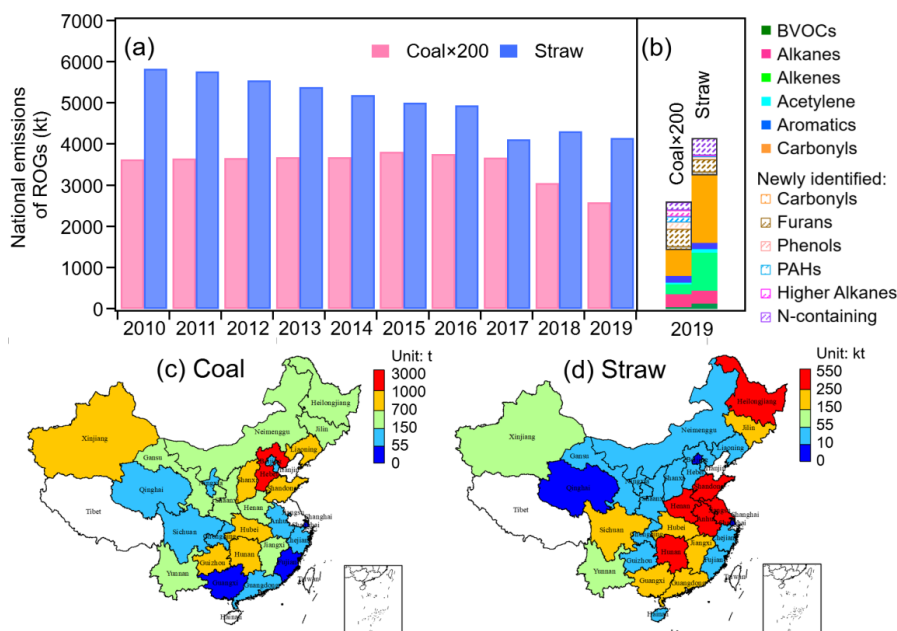
363

364 **Figure 4.** Emissions of ROGs from residential coal and straw combustion in China. (a)
365 Annual variation of national ROG emissions and (b) the speciation of ROG emissions
366 in 2019 from residential coal and straw combustion. The black boxes indicate the
367 emissions of newly identified species. (c, d) Spatial distribution of ROG emissions from
368 coal combustion in 2019 and straw combustion in 2017 respectively. The blank parts
369 on the map indicate the provinces with missing data.

370 **4. Conclusions**

371   In this study, a near-complete chemical description of ROGs emitted from
372 residential coal and biomass combustion was developed to get more insights into their
373 atmospheric effects. ROGs identified by the present method accounted for ~90% of the
374 "total" as the sum of species by Gas Chromatography equipped with a Mass
375 Spectrometer and a Flame Ionization Detector (GC-MS/FID) and H_3O^+/NO^+ Proton
376 Transfer Reaction Time-of-Flight Mass Spectrometer (Vocus PTR-ToF-MS). Among
377 the near-complete description of ROGs, 55 species un- and under-characterized in
378 previous studies using GC methods were analyzed intensively by Vocus PTR-ToF-MS,
379 mainly including oxygenated species (carbonyls, furans, phenols), higher hydrocarbons
380 (PAHs, higher alkanes) with carbon atoms more than 8 as well as nitrogen-containing
381 compounds.

382   For the nearly complete ROGs dividing into three categories by the element
383 composition, oxygenated species played a similar major role with hydrocarbons, and
384 nitrogen-containing species dominated by acetonitrile and acrylonitrile were also
385 considerable in ROG emissions from residential combustion. Especially, coal
386 combustion emitted considerable higher alkanes including 8–21 carbon atoms, gaseous
387 PAHs (mainly including 2–3 benzene rings), furans and phenols, differently biomass
388 combustion emitted more carbonyls and terpenes.

389   Considering the newly discovered species, it is observed that approximately half
390 and a quarter of the ROG emissions from coal and biomass combustion are
391 underestimated. Combining with the spatial-temporal consumption of residential coal
392 and biomass combustion in China, ROG emissions of residential combustion were
393 estimated. The ROG emissions from straw combustion were two orders of magnitude
394 higher than those from coal combustion with negligible decline in recent years as the

395   limited straw utilization ratio, which suggested the biomass combustion would be the
396   only important residential emissions with the continuous replacement of residential coal
397   in rural of China. Given the newly identified species more reactive or with higher SOA
398   yields, amplified underestimation of OHR and SOAP were observed for both coal
399   combustion (59.4% ± 4.8% and 89.2% ± 1.0%) and biomass combustion (26.2 ± 6.8%
400   and 70.3% ± 1.6%). These results highlighted the importance of the completely
401   speciated measurement of the ROG emissions from residential combustion.

402

403   **Data availability**

404   Data presented in this paper are freely accessible from the following link:
405   https://data.mendeley.com/datasets/z78zz7mv7h/1 (Mendeley Data, V1, doi:
406   10.17632/z78zz7mv7h.1, Wang et al., 2022)

407

408   **Competing interests**

409   The authors declare that they have no conflict of interest.

410

411   **Authors contributions.** All authors contributed to the manuscript and have given
412   approval of the final version. H.W. and C.H. designed the study. H.W. and Y.G.
413   performed the data analyses and wrote the manuscript. Y.G., L.Y., and S.J. conducted
414   the experiment. B.Y., G.S., Y.L., Q.W., D.H., S.Z., and S.L., contributed to the
415   interpretation of results. L.Z and A.K. revised the manuscript. S.T. assisted in sampling.

416

417   **Acknowledgments.** This work was supported by National Natural Science Foundation
418   of China (42175135) and the Science and Technology Commission of the Shanghai
419   Municipality (20ZR1447800).

References

Andreae, M. O.: Emission of trace gases and aerosols from biomass burning – an updated assessment, Atmos. Chem. Phys., 19, 8523-8546, 10.5194/acp-19-8523-2019, 2019.

Andreae, M. O.: Biomass Burning Emission Factors, https://edmond.mpdl.mpg.de/imeji/collection/op2vVE8m0us_gcGC, 2021.

Cai, S., Zhu, L., Wang, S., Wisthaler, A., Li, Q., Jiang, J., and Hao, J.: Time-Resolved Intermediate-Volatility and Semivolatile Organic Compound Emissions from Household Coal Combustion in Northern China, Environ. Sci. Technol., 53, 9269-9278, 10.1021/acs.est.9b00734, 2019.

Carter, W. P. L.: Reactivity Estimates for Selected Consumer Product Compounds. University of California, pp. 06-408, 2008.

Chang, X., Zhao, B., Zheng, H., Wang, S., Cai, S., Guo, F., Gui, P., Huang, G., Wu, D., Han, L., Xing, J., Man, H., Hu, R., Liang, C., Xu, Q., Qiu, X., Ding, D., Liu, K., Han, R., Robinson, A. L., and Donahue, N. M.: Full-volatility emission framework corrects missing and underestimated secondary organic aerosol sources, One Earth, 5, 403-412, 10.1016/j.oneear.2022.03.015, 2022.

Collard, F.-X. and Blin, J.: A review on pyrolysis of biomass constituents: Mechanisms and composition of the products obtained from the conversion of cellulose, hemicelluloses and lignin, Renewable and Sustainable Energy Reviews, 38, 594-608, 10.1016/j.rser.2014.06.013, 2014.

Du, W., Yun, X., Chen, Y., Zhong, Q., Wang, W., Wang, L., Qi, M., Shen, G., and Tao, S.: PAHs emissions from residential biomass burning in real-world cooking stoves in rural China, Environmental pollution (Barking, Essex : 1987), 267, 115592-115592, 10.1016/j.envpol.2020.115592, 2020.

Gao, Y., Wang, H., Liu, Y., Zhang, X., Jing, S., Peng, Y., Huang, D., Li, X., Chen, S., Lou, S., Li, Y., and Huang, C.: Unexpected high contribution of residential biomass burning to non-methane organic gases (NMOGs) in the Yangtze River Delta region of China, Journal of Geophysical Research: Atmospheres, n/a, e2021JD035050, https://doi.org/10.1029/2021JD035050, 2022.

Gilman, J. B., Lerner, B. M., Kuster, W. C., Goldan, P. D., Warneke, C., Veres, P. R., Roberts, J. M., de Gouw, J. A., Burling, I. R., and Yokelson, R. J.: Biomass burning emissions and potential air quality impacts of volatile organic compounds and other trace gases from fuels common in the US, Atmospheric Chemistry and Physics, 15, 13915-13938, 10.5194/acp-15-13915-2015, 2015.

Hatch, L. E., Yokelson, R. J., Stockwell, C. E., Veres, P. R., Simpson, I. J., Blake, D. R., Orlando, J. J., and Barsanti, K. C.: Multi-instrument comparison and compilation of non-methane organic gas emissions from biomass burning and implications for smoke-derived secondary organic aerosol precursors, Atmospheric Chemistry and Physics, 17, 1471-1489, 10.5194/acp-17-1471-2017, 2017.

Heald, C. L. and Kroll, J. H.: The fuel of atmospheric chemistry: Toward a complete

461 description of reactive organic carbon, Science Advances, 6, 10.1126/sciadv.aay8967,
462 2020.

463 Heald, C. L., Gouw, J. d., Goldstein, A. H., Guenther, A. B., Hayes, P. L., Hu, W.,
464 Isaacman-VanWertz, G., Jimenez, J. L., Keutsch, F. N., Koss, A. R., Misztal, P. K.,
465 Rappenglück, B., Roberts, J. M., Stevens, P. S., Washenfelder, R. A., Warneke, C., and
466 Young, C. J.: Contrasting Reactive Organic Carbon Observations in the Southeast
467 United States (SOAS) and Southern California (CalNex), Environ. Sci. Technol., 54,
468 14923-14935, 10.1021/acs.est.0c05027, 2020.

469 Huo, Y., Guo, Z., Li, Q., Wu, D., Ding, X., Liu, A., Huang, D., Qiu, G., Wu, M., Zhao,
470 Z., Sun, H., Song, W., Li, X., Chen, Y., Wu, T., and Chen, J.: Chemical Fingerprinting
471 of HULIS in Particulate Matters Emitted from Residential Coal and Biomass
472 Combustion, Environ Sci Technol, 55, 3593-3603, 10.1021/acs.est.0c08518, 2021.

473 Koss, A. R., Sekimoto, K., Gilman, J. B., Selimovic, V., Coggon, M. M., Zarzana, K.
474 J., Yuan, B., Lerner, B. M., Brown, S. S., Jimenez, J. L., Krechmer, J., Roberts, J. M.,
475 Warneke, C., Yokelson, R. J., and de Gouw, J.: Non-methane organic gas emissions
476 from biomass burning: identification, quantification, and emission factors from PTR-
477 ToF during the FIREX 2016 laboratory experiment, Atmos. Chem. Phys., 18, 3299-
478 3319, 10.5194/acp-18-3299-2018, 2018.

479 Lim, Y. B. and Ziemann, P. J.: Effects of Molecular Structure on Aerosol Yields from
480 OH Radical-Initiated Reactions of Linear, Branched, and Cyclic Alkanes in the
481 Presence of NOx, Environ. Sci. Technol., 43, 2328-2334, 10.1021/es803389s, 2009.

482 Liu, W.-J., Li, W.-W., Jiang, H., and Yu, H.-Q.: Fates of Chemical Elements in Biomass
483 during Its Pyrolysis, Chemical Reviews, 117, 6367-6398,
484 10.1021/acs.chemrev.6b00647, 2017.

485 Ministry of Ecology and Environment of the People's Republic of China, National
486 Bureau of Statistics, and Ministry of Agriculture and Rural Affairs of the People's
487 Republic of China: Second National Pollution Source Census Bulletin, 2020.

488 Mo, Z., Shao, M., and Lu, S.: Compilation of a source profile database for hydrocarbon
489 and OVOC emissions in China, Atmos. Environ., 143, 209-217,
490 10.1016/j.atmosenv.2016.08.025, 2016.

491 Morgan, T. J. and Kandiyoti, R.: Pyrolysis of Coals and Biomass: Analysis of Thermal
492 Breakdown and Its Products, Chemical Reviews, 114, 1547-1607, 10.1021/cr400194p,
493 2014.

494 National Bureau of Statistics: China Energy Statistical Yearbook.
495 https://navi.cnki.net/knavi/yearbooks/YCXME/detail., China Statistics Press2010-
496 2022.

497 National Development and Reform Commission: Planning for clean heating in winter
498 in northern China (2017-2021), http://www.gov.cn/xinwen/2017-
499 12/20/content_5248855.htm, 2017.

500 Ng, N. L., Kroll, J. H., Chan, A. W. H., Chhabra, P. S., Flagan, R. C., and Seinfeld, J.
501 H.: Secondary organic aerosol formation from m-xylene, toluene, and benzene, Atmos.
502 Chem. Phys., 7, 3909-3922, 2007.

503   Pagonis, D., Sekimoto, K., and de Gouw, J.: A Library of Proton-Transfer Reactions of
504   H3O(+) Ions Used for Trace Gas Detection, J Am Soc Mass Spectrom, 30, 1330-1335,
505   10.1007/s13361-019-02209-3, 2019.

506   Qianzhan Industrial Research Institute: Report of Prospects and Investment Strategy
507   Planning Analysis on China Straw Refuse Treatment Industry (2022-2027).
508   https://www.qianzhan.com/analyst/detail/220/210508-14a4546c.html,   2022.

509   Qu, H., Wang, Y., Zhang, R., Liu, X., Huey, L. G., Sjostedt, S., Zeng, L., Lu, K., Wu,
510   Y., Shao, M., Hu, M., Tan, Z., Fuchs, H., Broch, S., Wahner, A., Zhu, T., and Zhang, Y.:
511   Chemical Production of Oxygenated Volatile Organic Compounds Strongly Enhances
512   Boundary-Layer Oxidation Chemistry and Ozone Production, Environ Sci Technol, 55,
513   13718-13727, 10.1021/acs.est.1c04489, 2021.

514   Sekimoto, K., Li, S.-M., Yuan, B., Koss, A., Coggon, M., Warneke, C., and de Gouw,
515   J.: Calculation of the sensitivity of proton-transfer-reaction mass spectrometry (PTR-
516   MS) for organic trace gases using molecular properties, International Journal of Mass
517   Spectrometry, 421, 71-94, 10.1016/j.ijms.2017.04.006, 2017.

518   Stockwell, C. E., Veres, P. R., Williams, J., and Yokelson, R. J.: Characterization of
519   biomass burning emissions from cooking fires, peat, crop residue, and other fuels with
520   high-resolution proton-transfer-reaction time-of-flight mass spectrometry, Atmospheric
521   Chemistry and Physics, 15, 845-865, 10.5194/acp-15-845-2015, 2015.

522   Stockwell, C. E., Christian, T. J., Goetz, J. D., Jayarathne, T., Bhave, P. V., Praveen, P.
523   S., Adhikari, S., Maharjan, R., DeCarlo, P. F., Stone, E. A., Saikawa, E., Blake, D. R.,
524   Simpson, I. J., Yokelson, R. J., and Panday, A. K.: Nepal Ambient Monitoring and
525   Source Testing Experiment (NAMaSTE): emissions of trace gases and light-absorbing
526   carbon from wood and dung cooking fires, garbage and crop residue burning, brick
527   kilns, and other sources, Atmos. Chem. Phys., 16, 11043-11081, 10.5194/acp-16-
528   11043-2016, 2016.

529   Wang, C., Yuan, B., Wu, C., Wang, S., Qi, J., Wang, B., Wang, Z., Hu, W., Chen, W.,
530   Ye, C., Wang, W., Sun, Y., Wang, C., Huang, S., Song, W., Wang, X., Yang, S., Zhang,
531   S., Xu, W., Ma, N., Zhang, Z., Jiang, B., Su, H., Cheng, Y., Wang, X., and Shao, M.:
532   Measurements of higher alkanes using NO+ chemical ionization in PTR-ToF-MS:
533   important contributions of higher alkanes to secondary organic aerosols in China,
534   Atmos. Chem. Phys., 20, 14123-14138, 10.5194/acp-20-14123-2020, 2020a.

535   Wang, H., Lou, S., Huang, C., Qiao, L., Tang, X., Chen, C., Zeng, L., Wang, Q., Zhou,
536   M., Lu, S., and Yu, X.: Source Profiles of Volatile Organic Compounds from Biomass
537   Burning in Yangtze River Delta, China, Aerosol and Air Quality Research, 14, 818-828,
538   10.4209/aaqr.2013.05.0174, 2014.

539   Wang, H., Gao, Y., Wang, S., Wu, X., Liu, Y., Li, X., Huang, D., Lou, S., Wu, Z., Guo,
540   S., Jing, S., Li, Y., Huang, C., Tyndall, G. S., Orlando, J. J., and Zhang, X.: Atmospheric
541   Processing of Nitrophenols and Nitrocresols From Biomass Burning Emissions, Journal
542   of Geophysical Research: Atmospheres, 125, 10.1029/2020jd033401, 2020b.

543   Wang, W., Yuan, B., Peng, Y., Su, H., Cheng, Y., Yang, S., Wu, C., Qi, J., Bao, F.,
544   Huangfu, Y., Wang, C., Ye, C., Wang, Z., Wang, B., Wang, X., Song, W., Hu, W., Cheng,
545   P., Zhu, M., Zheng, J., and Shao, M.: Direct observations indicate photodegradable

oxygenated volatile organic compounds (OVOCs) as larger contributors to radicals and ozone production in the atmosphere, Atmos. Chem. Phys., 22, 4117-4128, 10.5194/acp-22-4117-2022, 2022.

Wu, C., Wang, C., Wang, S., Wang, W., Yuan, B., Qi, J., Wang, B., Wang, H., Wang, C., Song, W., Wang, X., Hu, W., Lou, S., Ye, C., Peng, Y., Wang, Z., Huangfu, Y., Xie, Y., Zhu, M., Zheng, J., Wang, X., Jiang, B., Zhang, Z., and Shao, M.: Measurement report: Important contributions of oxygenated compounds to emissions and chemistry of volatile organic compounds in urban air, Atmos. Chem. Phys., 20, 14769-14785, 10.5194/acp-20-14769-2020, 2020.

Yang, G., Zhao, H., Tong, D. Q., Xiu, A., Zhang, X., and Gao, C.: Impacts of post-harvest open biomass burning and burning ban policy on severe haze in the Northeastern China, Sci Total Environ, 716, 10.1016/j.scitotenv.2020.136517, 2020.

Yuan, B., Koss, A. R., Warneke, C., Coggon, M., Sekimoto, K., and de Gouw, J. A.: Proton-Transfer-Reaction Mass Spectrometry: Applications in Atmospheric Sciences, Chemical Reviews, 117, 13187-13229, 10.1021/acs.chemrev.7b00325, 2017.

Yun, X., Shen, G., Shen, H., Meng, W., Chen, Y., Xu, H., Ren, Y., Zhong, Q., Du, W., Ma, J., Cheng, H., Wang, X., Liu, J., Wang, X., Li, B., Hu, J., Wan, Y., and Tao, S.: Residential solid fuel emissions contribute significantly to air pollution and associated health impacts in China, Science Advances, 6, eaba7621, 10.1126/sciadv.aba7621, 2020.

Zarzana, K. J., Min, K.-E., Washenfelder, R. A., Kaiser, J., Krawiec-Thayer, M., Peischl, J., Neuman, J. A., Nowak, J. B., Wagner, N. L., Dube, W. P., St Clair, J. M., Wolfe, G. M., Hanisco, T. F., Keutsch, F. N., Ryerson, T. B., and Brown, S. S.: Emissions of Glyoxal and Other Carbonyl Compounds from Agricultural Biomass Burning Plumes Sampled by Aircraft, Environ. Sci. Technol., 51, 11761-11770, 10.1021/acs.est.7b03517, 2017.

Zhu, X., Yun, X., Meng, W., Xu, H., Du, W., Shen, G., Cheng, H., Ma, J., and Tao, S.: Stacked Use and Transition Trends of Rural Household Energy in Mainland China, Environ. Sci. Technol., 53, 521-529, 10.1021/acs.est.8b04280, 2019.